Longitudinal Jerk Estimation for Identification of Driver Intention

Andrea Bisoffi*, Francesco Biral*, Mauro Da Lio* and Luca Zaccarian*†
*Dipartimento di Ingegneria Industriale, University of Trento, Italy
†CNRS, LAAS and Université de Toulouse, 7 Avenue du Colonel Roche, 31077 Toulouse, France
Email: {andrea.bisoffi, francesco.biral, mauro.dalio}@unitn.it, zaccarian@laas.fr

***Abstract*—We address the problem of estimating online the longitudinal jerk desired by a human driver piloting a car. This estimation is relevant in the context of suitable identification of driver intentions within modern Advanced Driver Assistance Systems (ADAS) such as the co-driver scheme proposed by some of the authors. The proposed architecture is based on suitably combining a Kalman filter with a scaling technique peculiar of the context of "high-gain" observers. The scaling is appealing because it allows for an easy tuning of the trade-off between phase lag and sensitivity to noise of the resulting estimate. Additionally, we show that using engine-related experimental measurements available in the CAN bus, it is possible to provide a more reliable estimate of the driver-intended jerk, especially in the presence of gear changes. The proposed scheme shows very desirable results on experimental data from a track test, also when compared to a brute force approach based on a mere kinematic model.**

I. Introduction

The derivative of the acceleration, the jerk, has recently gained more attention within the automotive community, both for longitudinal and lateral dynamics, and some works that explicitly take the jerk in consideration are [23], [22] and [20], [13]. In the first three references, the jerk was used as a very informative signal to extract the strategy behind the driver maneuver. In particular, in [23] the behaviour of an expert driver was studied from the jerk viewpoint to come up with a new control strategy, and in [23, Sec. 2.2] the additional benefit of considering the jerk signal was pointed out as compared to using only the steering angle speed or the yaw angular acceleration. In [13] the jerk signal was monitored in order to check that the safety and comfort requirements were satisfied. A similar use of the jerk (monitoring) was made in the different context of CNC machines in [17].

Still, one of the main drawbacks when using the jerk is that jerk sensors are neither off-the-shelf nor widespread (although a jerk sensor is proposed in [21]). Therefore, jerk is typically obtained through suitable filtering of the acceleration like in [13, Sec. IV.B] or [23, Sec. 5.2] (see also the improved approaches proposed in [17] and [14]). A natural approach to obtain the jerk is then to estimate it by means of Kalman filtering, as done in [15], where the Kalman filtering scheme was tested in simulations. Another approach may be to use high-gain techniques for numerical differentiation, as in [6] and [4], and our approach could be seen as intermediate between the previous two since it employs acceleration measurement, in the context of asymptotic observers. Our work provides a jerk estimate validated on experimental data, and the estimation paradigm is a Kalman formulation enriched by a high-gain-inspired scaling. While in the typical high-gain approach the scaling parameter ℓ is taken large ("high"), we exploited here the key idea of using it to move the location of all the eigenvalues of the error dynamics (placed with a Kalman approach). In this way by means of the scalar knob ℓ suitable trade-offs between the convergence rate of the estimation error and the sensitivity to noise can be easily obtained.

Another strong motivation for this work is to bring the driver intention into the picture of jerk estimation problems. In contrast to standard approaches, like [12] and [16], the driver can be modeled within the conceptual framework of subsumptive control architectures (outlined in [3]), where low level optimized motor primitives are combined into more complex (*subsumptive*) behaviors to achieve strategic and tactical goals (for a review of driver modeling, see [5, Sec. II]). According to this subsumptive paradigm, a co-driver (defined in [5, Sec. I.A]) was developed within the European project interactIVe [1]. Intention inference is the key point in order to develop applications that properly warn or support the driver in his/her task. This is done by the co-driver using *actively* the estimated jerk $\hat{\jmath}$ of the vehicle, resulting from the driver current maneuver. In particular, based on the current state of the vehicle and the available information from the environment, the co-driver hypothesizes a set of different possible high-level maneuvers (generated by solving corresponding optimal control problems according to human-like objective functions) and assumes as current driver maneuver the one in the set whose jerk has the least mismatch with $\hat{\jmath}$. This is motivated by the fact that different high level maneuvers map to different jerk evolutions of the vehicle. The inference about the current maneuver is then naturally used to assess the associated level of risk and issue suitable warnings (as in the interactIVe project [1]) or intervene directly (as in the running adaptIVe project [2]). It is then evident that inaccurate jerk estimates may lead to dramatically wrong driver intention inferences and consequently to false or missed alarms, or worse, to wrong interventions. In light of this discussion we emphasize that we are interested in the jerk related to the longitudinal dynamics *as* it is *perceived by* the (typical) *human driver*. In this sense (intention-oriented jerk estimate) the current work improves upon the jerk estimation algorithms of [5] (to which our work is intimately related), and will enhance the current co-driver scheme.

The paper is organized as follows. In Section II the model for the longitudinal dynamics of the vehicle is presented and the torque request signal is introduced, which is fundamental to capture the driver intention. Based on the difference between the torque request and the engine torque, we build in Section III our intention-oriented model for the jerk signal. This model is cast into a Kalman formulation in Section IV, where we also introduce a high-gain-like enhancement starting from

the Kalman formulation. In Section V the intention-oriented approach is validated on experimental data from a track test. Section VI concludes the paper and outlines future work.

II. Longitudinal vehicle dynamics and driver intention

Consider (from Newton's equation) the following standard model for the longitudinal dynamics:

$$M\dot{v} = \tau T_e - \underbrace{Mg\sin\alpha}_{=:F_s} - \underbrace{C_r Mg\cos\alpha}_{=:F_f} - \underbrace{\frac{1}{2}\varrho S C_x v^2}_{=:F_d} \qquad (1)$$

where v and α are respectively the longitudinal velocity of the vehicle and the road slope, F_s, F_f and F_d are respectively the dissipative forces due to the road slope, friction and aerodynamic drag, τT_e is the force actuated by the engine and transmitted to the wheels via gearbox and driveline, with transmission coefficient τ corresponding to:

$$\tau = \frac{1}{r_r}\eta_g\eta_d\tau_g\tau_d, \qquad (2)$$

and finally all other physical parameters are listed in Table I.

Parameter	Symbol
Vehicle mass	M
Rolling radius	r_r
Gearbox efficiency	η_g
Driveline efficiency	η_d
Gearbox transmission ratio	τ_g
Driveline transmission ratio	τ_d
Gravity	g
Rolling friction coefficient	C_r
Air density	ϱ
Reference area	S
Drag coefficient	C_x

Table I: Physical parameters for the longitudinal dynamics.

A few notes are in order: (i) because of the term $C_r Mg\cos\alpha$, the model (1) is valid only when the vehicle is moving. (ii) The gearbox transmission ratio τ_g depends on the specific gear engaged, but it is assumed that the latter is known from the electronic control unit (ECU) as a function of time. (iii) The parameters C_r and $\varrho S C_x$, which are typically known with a high degree of uncertainty (e.g., variations in the vertical loads, tire wear and inflation), are stated here only for the sake of explanation, but their knowledge is *not* needed for estimating the driver's desired acceleration and jerk, as we will point out in Remark 2. (iv) Due to space constraints we only consider the engine traction torque T_e, but the braking action could be similarly obtained by way of suitable coefficients from the brake pressure.

It is reasonable to assume that the road slope α is sufficiently small (less than 10°) in most urban and extra-urban roads that do not involve mountain routes, so that we may approximate (1) as

$$M\dot{v} = \tau T_e - Mg\alpha - C_r Mg - \frac{1}{2}\varrho S C_x v^2, \qquad (3a)$$

and the validity of this assumption on α in our study can be checked *a posteriori* directly on the data themselves as per Figure 1. Alternatively, the analysis carried out here can be repeated by replacing state α with another state $s_\alpha = \sin(\alpha)$.

Measured quantities come from accelerometers and odometers. The measured acceleration from the accelerometer is

$$y_1 = \dot{v} + g\sin\alpha + \bar{d}_a \approx \dot{v} + g\alpha + \bar{d}_a, \qquad (3b)$$

which illustrates that the accelerometer measures not only the derivative $\dot{v}$ of the longitudinal velocity, but it is also affected by the road slope and by a bias term $\bar{d}_a$ due to a possible (static) misalignment of the sensor. As from (1) to (3a), $\sin\alpha$ has been again approximated by α. The longitudinal vehicle velocity that we consider as output is

$$y_2 = v, \qquad (3c)$$

and is obtained as the product between the rolling radius r_r and the average of the rotational velocities of the two non-traction wheels, because these velocities are less prone to slip phenomena (for this practice see, e.g., [18] or [11, Sec. 2.4]). We did not want to model the longitudinal slip in this work mainly because the *typical* human driver neither perceives this type of dynamics nor can control it (see the motivations behind the introduction of traction control and ABS in, e.g., [8]) and here we are interested in a driver-oriented modeling. The wheels rotational velocities are measured by odometers.

Remark 1: A number of phenomena that have mild effects on the longitudinal dynamics (as resulting from a typical human driver) have been neglected here: among them, suspensions and pitch motion, load transfer, interactions with the road and lateral dynamics. In Section IV, these effects will be taken into account by lumping them into appropriate noise terms. ⌟

To embed the driver intention in the longitudinal dynamics model (3a), we first need to bring the driver's torque request into the picture. To this end, we first note that the considered vehicle operates with a robotized gearbox and electronic clutch that may modify the requested torque to adapt to operating conditions. In modern vehicles, the driver provides the ECU with a torque *r*equest, T_r, by acting on the throttle pedal. In most cases, the ECU complies with the driver's torque request T_r and exerts it on the engine (if one neglects the engine dynamics that is far faster than the mechanical dynamics in (3a)). However, sometimes the ECU intervenes enacting a torque that is computed according to the ECU's own logic (which is unknown to us), based on the whole state of the engine and of the powertrain (and not only based on slower time-scale quantities, as the driver does). Typical cases when this decoupling occurs are gear changes, when the ECU smooths out the transition between the actual gears via direct control of the engine torque, or when standard Active Vehicle Control Systems intervene, like ABS or ESP. A couple of illustrative transitions when a gear change takes place will be represented in Figure 3 in Section V, where the signals T_r and T_e will be displayed.

The key aspect that allows us for the following intention-oriented modeling is that both signals T_r and T_e are measurable on the CAN bus of the vehicle, which is a common feature in modern vehicles. In this sense, the decoupling induced by the ECU can be thought of as a torque disturbance T_d that is obtained from signals T_e and T_r as

$$T_r + T_d = T_e,$$

where T_d denotes a measurable disturbance, so that intuitively it accounts for all the torque generation dynamics that are

too fast for the human driver to control, i.e. beyond his/her actuation capabilities, while T_r reflects the driver intention.

If the driver's requested torque T_r were actuated by the engine with no in-between interposition, then, following (3a), we would have

$$M\dot{v}_i = \tau T_r - Mg\alpha - C_r Mg - \frac{1}{2}\varrho S C_x v^2. \tag{4}$$

According to this equation, v_i is the travel speed of the vehicle that would be obtained resulting from mere driver's actuation, which we call intended speed, after the *actual* F_s, F_f, F_d of (1) are subtracted from τT_r.

III. Intention-oriented model

In this Section we state the equations of our intention-oriented model, and we provide the kinematic model used in [5] as a means of comparison in Remark 3.

Although we introduced the insightful Equation (4) for the intended speed v_i and in the following we will use quantities that are derived from v_i (namely the intended acceleration and jerk, a_i and $\bar{j}_i$), we do *not* want to include v_i as state variable. The state vector we are going to define is instead $x_i = [v \quad a_i \quad o_a \quad \bar{j}_i]^T$.

From the intended speed v_i, the intended acceleration and jerk are defined from classical mechanics as $a_i = \dot{v}_i$ and $\bar{j}_i = \dot{a}_i$, respectively.

Combine (3a) and (4), obtaining

$$\underbrace{M\dot{v}}_{:=Ma} = \tau(T_e - T_r) + \underbrace{M\dot{v}_i}_{:=Ma_i}, \tag{5}$$

and define the accelerometer offset o_a as

$$o_a = g\alpha + \bar{d}_a, \tag{6}$$

i.e. as the sum of the two effects (static misalignment and slope) that prevent the accelerometer measurement in (3b) from being exactly the derivative of the longitudinal velocity. From (5), using the definition $a_i = \dot{v}_i$, we get

$$\dot{v} = a_i + \frac{\tau}{M}(T_e - T_r), \tag{7a}$$

which is our first state equation. Then the jerk definition yields

$$\dot{a}_i = \bar{j}_i. \tag{7b}$$

Consider the dynamics of o_a in (6): for the term $\bar{d}_a$ we have that $\dot{\bar{d}}_a = 0$ is true except from very slow drifts (e.g., temperature-related) while for α, we still write $\dot{\alpha} = 0$ since the slope is slowly time varying as compared to the dynamics of mechanical quantities like v, v_i etc. (for this practice in slope estimation see, e.g., [18, Eq. (13)]). Thus

$$\dot{o}_a = 0, \tag{7c}$$

for which a note is in order. The plant model (7a)-(7d) will be used in a Kalman-like estimator in Section IV, and state equation noise terms Δv, Δa_i, Δo_a, $\Delta \bar{j}_i$ will be added respectively to Equations (7a), (7b), (7c), (7d). As it is standard practice in Kalman filters, the introduction of a high variance for the noise Δo_a takes into account the intrinsic unreliability of (7c), which otherwise would imply that the slope is constant even though the actual slope is slowly time-varying.

Finally, we consider for the intended jerk:

$$\dot{\bar{j}}_i = 0, \tag{7d}$$

which is motivated by the following considerations. (i) A first intuition is that drivers tend to settle to a constant value of the pedal (which reflects their intentions) if the traffic scenario remains unchanged, but they act linearly on the pedal with respect to time when the scenario changes. (ii) As already noted for Equation (7c), we do *not* claim that the model $\dot{\bar{j}}_i = 0$ is *exact*, indeed we take into account approximations by suitable variances selections comprising, e.g., that (7d) is less reliable than (7a) and (7b), especially when the traffic scenario changes and the driver pursues another high level maneuver. Thus, the variance of noise $\Delta\bar{j}_i$ will be larger than those of Δv and Δa_i in our Kalman-like estimator. (iii) Experimental evidence shows that the optimal feedback control laws for typical motor tasks obey a "minimal intervention" principle where inaccuracies of the executed motion are corrected only when they interfere with the task goals (see, e.g., [19] and [22]).

With the choice of state variables $x_i = [\, v \; a_i \; o_a \; \bar{j}_i \,]^T$, it is straightforward to reformulate measurements (3b) and (3c) as a suitable linear output:

$$y_1 = a_i + \frac{\tau}{M}(T_e - T_r) + o_a \tag{7e}$$

$$y_2 = v \tag{7f}$$

using (5) and definition (6) for the accelerometer offset o_a.

Remark 2: From Equations (7) it is evident that the *only* physical parameters we are required to know beforehand according to this formulation are the transmission coefficient τ in (2) and the vehicle mass M. Moreover, the nonlinearities due to aerodynamic drag force F_d in (3a) disappear. ⌟

Since Equations (7b), (7d) involve quantities that are derived from the intended speed v_i and in (7e) Equation (5) (descending in turn from (4)) was directly employed, this should motivate why we claim that our jerk estimate $\bar{j}_i$ accounts for the driver intentions.

Remark 3: The following kinematic model is stated here mainly as a means of comparison with the previous intention-oriented model and was implemented in [5, Eq. (27)] to obtain an estimate of the longitudinal jerk. We will see in Section V to which extent the intention-oriented model improves the kinematic model. Using o_a in (6) again, the state equations are

$$\dot{v} = a \tag{8a}$$

$$\dot{a} = \bar{j} \tag{8b}$$

$$\dot{o}_a = 0 \tag{8c}$$

$$\dot{\bar{j}} = 0, \tag{8d}$$

with the same motivations behind Equations (8c) and (8d) as the ones behind Equations (7c) and (7d), respectively. In the three Equations (8a), (8b) and (8d), that correspond to a triple integrator, v, a and $\bar{j}$ are the effective kinematic quantities of the vehicle considered as a point mass, hence the name of this model, and do *not* embed any information about the driver intentions. Measurements (3b) and (3c) are reformulated as

$$y_1 = a + o_a \tag{8e}$$

$$y_2 = v. \tag{8f}$$

using the state $x_k = \begin{bmatrix} v & a & o_a & \bar{\jmath} \end{bmatrix}^T$ and (6). ⌟

IV. State estimation of jerk in an enhanced Kalman approach

In this Section we first introduce a Kalman formulation for the state estimator of the jerk, and second we will enhance that scheme using a high-gain-inspired scaling parameter ℓ, which serves as tuning knob for a suitable trade-off between the phase lag and the noise filtering action of the observer.

A. Kalman formulation

One can check trivially that Equations (7) and (8) can be *both* represented as the *linear* dynamical system

$$\dot{x}_m = Ax_m + B_m u \tag{9a}$$
$$y = Cx_m + D_m u, \tag{9b}$$

where the index $m \in \{i, k\}$ stands either for *i*ntention-oriented or *k*inematic model, so that

$$u = T_e - T_r, \quad x_i = \begin{bmatrix} v & a_i & o_a & \bar{\jmath}_i \end{bmatrix}^T, \quad x_k = \begin{bmatrix} v & a & o_a & \bar{\jmath} \end{bmatrix}^T \tag{10}$$

and then, from (7) and (8)

$$\left[\begin{array}{c|c|c} A & B_i & B_k \\ \hline C & D_i & D_k \end{array}\right] = \left[\begin{array}{cccc|c|c} 0 & 1 & 0 & 0 & \tau/M & 0 \\ 0 & 0 & 0 & 1 & 0 & 0 \\ 0 & 0 & 0 & 0 & 0 & 0 \\ 0 & 0 & 0 & 0 & 0 & 0 \\ \hline 0 & 1 & 1 & 0 & \tau/M & 0 \\ 1 & 0 & 0 & 0 & 0 & 0 \end{array}\right]. \tag{11}$$

Output y remains clearly the same physical quantity for both models $m = i$ or $m = k$, even though it is generated in a different way starting from x_i and u or from x_k. Note that the two models share the same matrices A and C.

Since in the design of the observer gain L in (14) only matrices A and C play a role, the coincise formulation in (9) allows us to carry out a single design procedure for *both* models (7) and (8). The whole following observer tuning is sound in light of the observability of pair (C, A) (see, e.g., [9]).

Remark 4: If we were to choose the state as $x_i = \begin{bmatrix} v & a_i & \alpha & \bar{d}_a & \bar{\jmath}_i \end{bmatrix}^T$ with $\dot{\alpha} = 0$, $\dot{\bar{d}}_a = 0$ and $y_1 = a_i + \frac{\tau}{M}(T_e - T_r) + g\alpha + \bar{d}_a$ (giving rise to matrices $\tilde{A}$, $\tilde{B}$, $\tilde{C}$, $\tilde{D}$), we would lose the observability of pair $(\tilde{C}, \tilde{A})$. In particular, contributions α and $\bar{d}_a$ cannot be distinguished from one another at the output. The same would hold in the case of the kinematic model. Nonetheless, distinguishing between the two is not necessary for the current type of application. ⌟

According to a Kalman formulation, we introduce suitable noise terms Δ_x and Δ_y on the state and output equations of (9), obtaining

$$\dot{x}_m = Ax_m + B_m u + \Delta_x \tag{12a}$$
$$y = Cx_m + D_m u + \Delta_y, \tag{12b}$$

where the covariance matrices of Δ_x and Δ_y are (using the expected value $E[\cdot]$)

$$Q = E[\Delta_x \Delta_x^T], \quad R = E[\Delta_y \Delta_y^T] \tag{13}$$

and the corresponding observer structure for (12) is

$$\dot{\hat{x}}_m = A\hat{x}_m + B_m u + L[y - C\hat{x}_m - D_m u] \tag{14}$$

where $\hat{x}_m$ is the estimate of state x_m.

As from Kalman theory, Q and R in (13) are known parameters but their identification is a cumbersome process (some approaches are summarized in [7, Introduction]). A more pragmatical approach is to consider diagonal Q, R and regard their elements on the diagonal as design parameters (see, e.g. [9, page 229]) that can account for how trustworthy the corresponding state or output equation is. This kind of approach was explained after (7c) and (7d) assuming $\Delta_x = \begin{bmatrix} \Delta v & \Delta a_i & \Delta o_a & \Delta \bar{\jmath}_i \end{bmatrix}^T$. This pragmatical approach may be seen legitimately as a way of tuning the observer gain L using Linear Quadratic techniques, that indeed make use of matrices Q and R, instead of, for instance, pole placement techniques.

In conclusion, given the plant matrices A and C and the "design" parameters Q and R, solving the algebraic Riccati equation allows tuning a gain

$$L_K = \begin{bmatrix} L_{va} & L_{vv} \\ L_{aa} & L_{av} \\ L_{oa} & L_{ov} \\ L_{ja} & L_{jv} \end{bmatrix} \tag{15}$$

that places the eigenvalues of $A - L_K C$ in a specific location and will be further employed in IV-B.

Consider the estimation error $\tilde{x}_m = x_m - \hat{x}_m$ between the true state in the Kalman formulation (12) and its estimate (14). The dynamics of $\tilde{x}_m$ can be conveniently written as follows in the absence of external perturbations:

$$\dot{\tilde{x}}_m = (A - LC)\tilde{x}_m. \tag{16}$$

If we select $L = L_K$, positive definiteness of Q and R imply that all eigenvalues $A - L_K C$ have negative real part. We will suitably scale this error dynamics in the next section by proposing a parametrized selection of L, based on L_K.

B. "High"-gain enhancement

This subsection deals with finding a convenient selection for matrix L in (14) that combines the Kalman approach (that has led to the gain L_K in (15)) and the need of a single tuning knob ℓ that allows to easily obtain a trade-off between the tracking speed and the noise rejection in the estimates.

From the error $\tilde{x}_m = \begin{bmatrix} \tilde{v} & \tilde{a}_m & \tilde{o}_a & \tilde{\bar{\jmath}}_m \end{bmatrix}^T$ (as before, a_m or $\bar{\jmath}_m$ are a_i or $\bar{\jmath}_i$ for the intention-oriented model and a or $\bar{\jmath}$ for the kinematic model) define the "high"-gain scaled error as

$$e = \begin{bmatrix} v \\ \frac{a_m}{\ell} \\ \frac{o_a}{\ell} \\ \frac{\bar{\jmath}}{\ell^2} \end{bmatrix} = \begin{bmatrix} 1 & & & \\ & \frac{1}{\ell} & & \\ & & \frac{1}{\ell} & \\ & & & \frac{1}{\ell^2} \end{bmatrix} \tilde{x}_m. \tag{17}$$

Remark 5: The name "high"-gain is motivated by the fact that a similar scaling in the inverse powers of a coefficient ℓ takes place in high-gain observers (for a full perspective on high-gain observers see, e.g., [10]). Historically, the parameter ℓ was chosen large (or "high") to dominate over the effect of uncertain or known nonlinearities. Here the parameter ℓ can be chosen large to increase the speed of convergence if L_K was tuned too conservatively, or small to improve the filtering action of the observer with respect to the action of noise: these two possibilities are exemplified in Section V. ⌟

The selection for L is

$$L = \begin{bmatrix} 1 & & \\ & \ell & \\ & & \ell^2 \end{bmatrix} L_K \begin{bmatrix} 1 \\ \ell \end{bmatrix} \tag{18}$$

Using (17), (18) and (16), it can be straightforwardly verified, after some calculations, that the dynamics for the scaled error e is given by

$$\dot{e} = \ell(A - L_K C)e, \tag{19}$$

which reveals that the eigenvalues of the scaled error dynamics are exactly the eigenvalues "placed" with the Kalman approach in Section IV-A for the matrix $A - L_K C$, scaled altogether in the complex plane by the factor ℓ. Error $\tilde{x}_m$ undergoes the same change in its dynamics because it is related to ℓ by the similarity transformation in (17). Once the baseline gain L_K is fixed, tuning ℓ allows for shifting in the left-half plane the whole set of the observer eigenvalues to the right (better rejection) or to the left (better tracking) as compared to their original positions. It is emphasized that this shifting is obtained by acting on *one* parameter *only*. We note that the scaled dynamics (19) could be obtained thanks to the peculiar structure of matrices A and C.

Remark 6: The intuition behind the chosen scaling of error in (17) is the customary one adopted in the high-gain scaling domain. Since (a subpart of) dynamic matrix A corresponds to a triple integrator, subsequent states are related by a simple integral relation (except for the jerk). Then appropriate scaling of the roots of the characteristic polynomial of the error dynamics is obtained by using in its coefficients increasing powers of the scaling factor. This is why the scaled error in (17) is necessary for a suitable representation. Finally, o_a could be scaled arbitrarily but it is convenient to scale it in the same way as the accelerations a_i or a because they are algebraically correlated in the output equation. ⌟

V. Validation on Experimental Test

The validation of the estimation approach in Section IV was performed on experimental data collected on a test track. The track test consisted of two laps, and was mainly designed to check the validity of this estimation approach in the case of normal driving of a typical human (in particular away from maneuvrability limits) since we are interested in inferring driver intentions in a *continuous* way and in the context of preventive safety. In this sense (i) the current study was preliminary and clarifies the possible use of this estimation approach within the (semi)autonomous-driving context of the European project adaptIVe [2], (ii) even if the performance of our jerk estimation was analyzed offline, our filtering scheme is as such *apt* for future *online usage*. The values for the parameters are $M = 1500$ kg, and $\tau_1 = 13$, $\tau_2 = 6.9$, $\tau_3 = 4.3$, $\tau_4 = 3.1$, $\tau_5 = 2.5$, where the subscript corresponds to the engaged gear. As mentioned in Section II the vehicle is equipped with a robotized gearbox and an electronic clutch. The matrices in (13) were chosen as

$$Q = \begin{bmatrix} 10^{-8} & & & \\ & 10^{-6} & & \\ & & 10^{-2} & \\ & & & 1 \end{bmatrix}, \quad R = \begin{bmatrix} 1 & \\ & 10^{-3} \end{bmatrix}. \tag{20}$$

Mainly to illustrate the whole dataset, we depict in Figure 1 the quantity $\frac{\hat{o}_a}{g}\frac{180^\circ}{\pi}$, i.e. the (normalized) estimated accelerometer offset converted in degrees. The light blue parts correspond to the time intervals when a gear change occurs: the darker areas correspond to the times when the clutch is disengaged from the engine, the lighter areas correspond to re-engagement. The periodicity in the depicted signal is related to the two

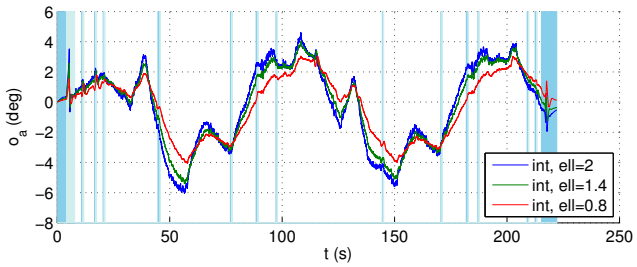

Figure 1: (Normalized) estimated offset $\hat{o}_a$ for the intention-oriented (int) model for different values of knob ℓ (ell).

track laps. The three different curves correspond to the three different values of $\ell = 2,\ 1.4,\ 0.8$.

In Figure 2, we present the three most relevant quantities, based on which we comment the jerk estimate that we can provide. At the top of the figure we have the estimated velocity $\hat{v}$, together with the measurement y_2 in (7f), which is barely distinguishable from the estimates. In the middle of the figure we have the intended acceleration $\hat{a}_i$ together with the measurement y_1 in (7e): the estimates differ from the measurement because of the direct feed-through from the input $u = T_e - T_r$. The difference $T_e - T_r$ bears not only the torque smoothing operated by the ECU (as pointed out in Section II) but also all the dissipation torques induced *within* the engine by the fluidodynamic and mechanical forces (engine friction). The latter account for the slowly time varying offset visible in the middle plot. Already from the middle plot, but even more from the bottom plot, the smoothening effect of parameter ℓ is evident. We would like to emphasize that with the parameter ℓ at hand, we could set the values of matrices Q and R in (20) based on high level considerations (the entries of Q reflect the fact that the first state equation is the most reliable one, as noted in Section III, while the ones in R that the measurements from the odometers are more reliable, as compared to the measurements from the accelerometers, in the considered application) and then readily adjust the filtering action through ℓ (small ℓ means large noise rejection at the cost of introducing a larger time-delay in the estimation). In this sense we partially overcome a commonly perceived limitation in the Kalman approach, i.e. that the covariance matrices are unknown in most cases. Let us comment on the effectiveness of the jerk estimate in the bottom diagram. As a first approximation, the velocity can be considered piecewise linear, giving rise to acceleration steps: thus the jerk signal is typically zero, which is consistent with the minimum intervention principle [22]. Even in the presence of noise, the essence of the maneuver is caught by the jerk estimate: in particular notice the amplitude slightly different from zero between 80 s and 87 s that justifies the mild drift in the acceleration. The relevant intention changes of the driver occur at about 78 s, 88 s, 102 s, when s/he sets off an acceleration phase, then leaves the car coasting, and finally accelerates again. All these changes are well captured by the jerk estimate presenting some bumps at the relevant times.

To show how the intention-oriented model improves upon the kinematic model of Remark 3, we present two gear changes in Figure 3, where in addition to the quantities of Figure 2 we plotted the signals T_e, T_r and the signal $\frac{\tau}{M}u = \frac{\tau}{M}(T_e - T_r)$,

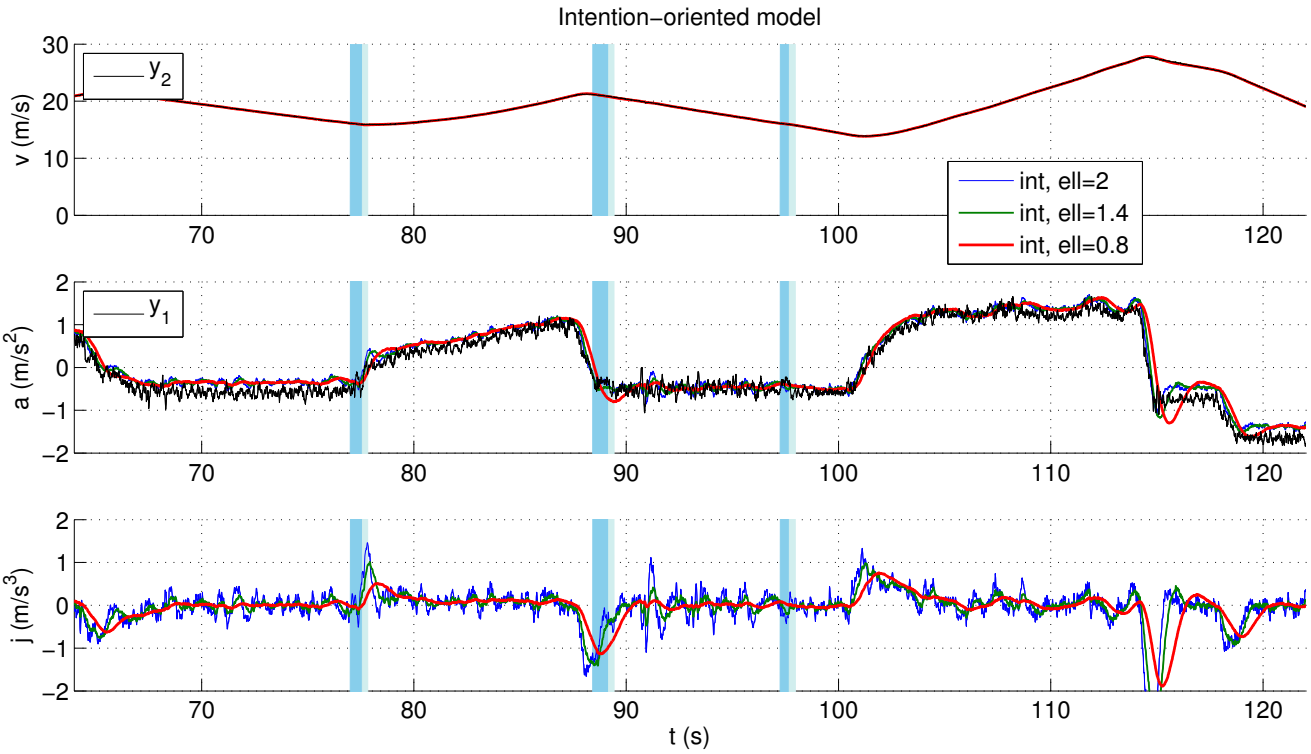

Figure 2: State estimates $\hat{v}$ (top, together with measurement y_2), $\hat{a}_i$ (middle, together with measurement y_1), $\hat{\dot{j}}_i$ (bottom) for the intention-oriented model (7) and three different values of ℓ.

that accounts for the driver intention. In the gear change at 171 s, the driver is still letting the car coasting, as witnessed by the evolution of the velocity (which decreases until 172 s), of the acceleration, and of the requested torque (which remains flat until 172 s). Therefore, no change of the intention is taking place in the driver's understanding until 172 s. This calls for the almost-flat jerk estimate (red dashed line). According to the decreasing velocity, the ECU decides to engage a lower gear and, to smooth the consequent re-engagement, induces a small burst in the engine torque (top plot). This causes a temporary acceleration of the vehicle, that is detected by the accelerometer. Therefore, if we used the kinematic model and its jerk estimate to infer the driver intentions, the process relative to the gear change would be misinterpreted and (erroneously) credited to driver intentions, resulting in a $\sim$-shaped evolution at 171 s in the jerk estimate (blue solid line). Specular considerations can be made for the gear change at 145 s, where the effectiveness of the jerk estimate of the intention-oriented model lies in the fact that the jerk estimate remains negative just after the gear change, while at that point the kinematic model produces a remarkably positive (and erroneous) estimate. This estimate would be erroneous from the viewpoint of the intentions because it is in contrast with the maneuver (constant velocity, and then deceleration) the driver carries out immediately after, between 145 s and 148 s.

VI. Conclusion and Future Work

In this paper we employed effectively the torque request signal (available on the CAN bus of modern vehicles) to perform a driver-intention oriented estimation of the longitudinal jerk signal. The interest in the longitudinal jerk is motivated by the fact that (i) typical drivers tend to map high-level maneuvers into different jerk evolutions, (ii) a newly devised ADAS (co-driver) based on the jerk signal was already implemented in the European project interactIVe. The structure of the proposed jerk estimator is based on a Kalman formulation, but we added a knob (inspired by high-gain scaling techniques) to suitably tune a trade-off between tracking speed and noise rejection in the resulting estimates. Finally, we validated the effectiveness of our jerk estimation on experimental signals. In future work, the improvements that we showed here in terms of compliance with the driver intentions will be illustrated in the co-driver architecture. Future work also includes using this same estimation paradigm (with scaling) for the lateral dynamics, where nonlinear effects can not be neglected. To this end, parameter ℓ could be tuned online according to a suitable adaptation logic. Another topic that we want to further study is to trace back the driver intentions analyzing directly throttle and brake pedals information, like pressures or positions.

Acknowledgment

The research leading to these results has received funding from the European Commission 7th Framework Programme under the project adaptIVe [2], grant agreement no. 610428. The authors would like to thank all partners within adaptIVe for their cooperation and valuable contribution. The work has also been supported by the University of Trento, grant OptHySYS. The authors would also like to thank Giulio Panzani for useful discussions.

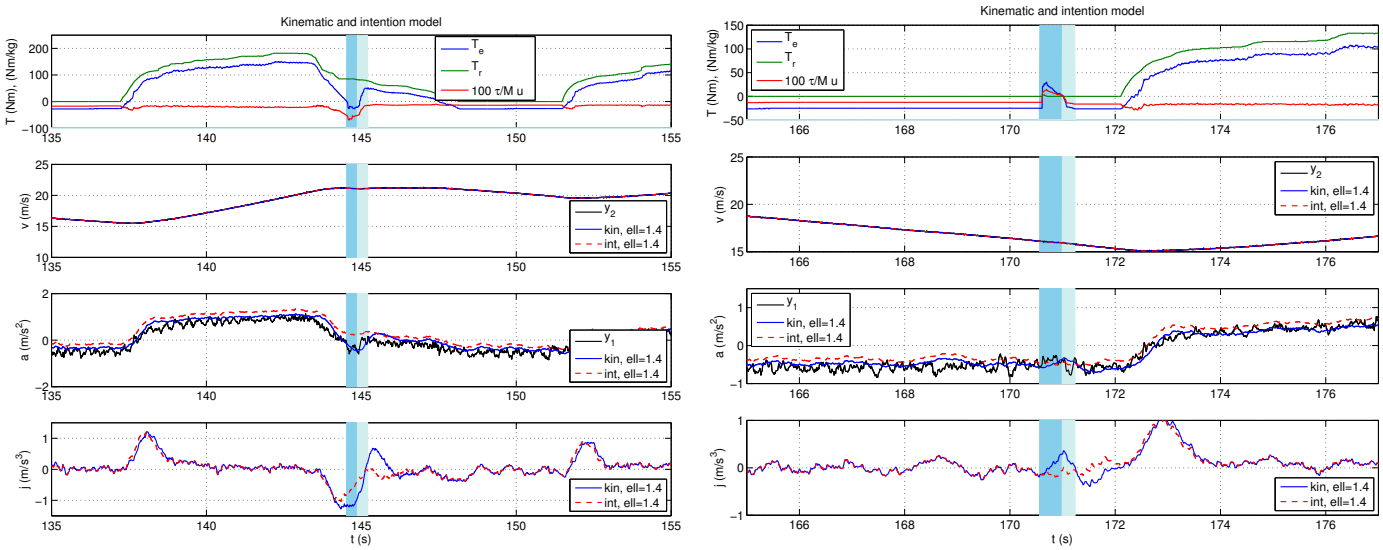

Figure 3: Illustrative transitions corresponding to two gear changes for the intention-oriented model (7) and the kinematic one (8) with fixed $\ell = 1.4$: torque signals T_e, T_r, $\frac{\tau}{M}u$ (first from top), $\hat{v}$ and y_2 (second), $\hat{a}_i$, a and y_1 (third), $\hat{\tilde{j}}_i$ and $\hat{\tilde{j}}$ (fourth).

REFERENCES

[1] "interactIVe: accident avoidance by intervention for Intelligent Vehicles," Online resource, 2010-2013, available at http://www.interactive-ip.eu/ [Accessed April 26, 2015].

[2] "adaptIVe: Automated Driving Applications and Technologies for Intelligent Vehicles," Online resource, 2014-, available at http://www.adaptive-ip.eu/ [Accessed April 26, 2015].

[3] R. Brooks, "A robust layered control system for a mobile robot," *Robotics and Automation, IEEE Journal of*, vol. 2, no. 1, pp. 14–23, 1986.

[4] Y. Chitour, "Time-varying high-gain observers for numerical differentiation," *Automatic Control, IEEE Transactions on*, vol. 47, no. 9, pp. 1565–1569, 2002.

[5] M. Da Lio, F. Biral, E. Bertolazzi, M. Galvani, P. Bosetti, D. Windridge, A. Saroldi, and F. Tango, "Artificial co-drivers as a universal enabling technology for future intelligent vehicles and transportation systems," *Intelligent Transportation Systems, IEEE Transactions on*, vol. 16, no. 1, pp. 244–263, 2015.

[6] A. M. Dabroom and H. K. Khalil, "Discrete-time implementation of high-gain observers for numerical differentiation," *International Journal of Control*, vol. 72, no. 17, pp. 1523–1537, 1999.

[7] S. Formentin and S. Bittanti, "An insight into noise covariance estimation for Kalman filter design," in *19th World Congress of the International Federation of Automatic Control*, vol. 19, no. 1, 2014, pp. 2358–2363.

[8] G. F. Fowler, R. E. Larson, and L. A. Wojcik, "Driver crash avoidance behavior: Analysis of experimental data collected in NHTSA's vehicle antilock brake system (ABS) research program," SAE Technical Paper, Tech. Rep., 2005.

[9] J. P. Hespanha, *Linear Systems Theory*. Princeton, New Jersey: Princeton Press, 2009.

[10] H. K. Khalil and L. Praly, "High-gain observers in nonlinear feedback control," *International Journal of Robust and Nonlinear Control*, vol. 24, no. 6, pp. 993–1015, 2014.

[11] M. Klomp, Y. Gao, and F. Bruzelius, "Longitudinal velocity and road slope estimation in hybrid electric vehicles employing early detection of excessive wheel slip," *Vehicle System Dynamics*, vol. 52, no. sup1, pp. 172–188, 2014.

[12] C. C. Macadam, "Understanding and modeling the human driver," *Vehicle System Dynamics*, vol. 40, no. 1-3, pp. 101–134, 2003.

[13] J.-J. Martinez and C. Canudas-de Wit, "A safe longitudinal control for adaptive cruise control and stop-and-go scenarios," *Control Systems Technology, IEEE Transactions on*, vol. 15, no. 2, pp. 246–258, 2007.

[14] L. Morales-Velazquez, R. de Jesus Romero-Troncoso, R. A. Osornio-Rios, and E. Cabal-Yepez, "Sensorless jerk monitoring using an adaptive antisymmetric high-order FIR filter," *Mechanical Systems and Signal Processing*, vol. 23, no. 7, pp. 2383 – 2394, 2009.

[15] S.-i. Nakazawa, T. Ishihara, and H. Inooka, "Real-time algorithms for estimating jerk signals from noisy acceleration data," *International Journal of Applied Electromagnetics and Mechanics*, vol. 18, no. 1, pp. 149–163, 2003.

[16] M. Plöchl and J. Edelmann, "Driver models in automobile dynamics application," *Vehicle System Dynamics*, vol. 45, no. 7-8, pp. 699–741, 2007.

[17] J. J. Rangel-Magdaleno, R. J. Romero-Troncoso, R. A. Osornio-Rios, and E. Cabal-Yepez, "Novel oversampling technique for improving signal-to-quantization noise ratio on accelerometer-based smart jerk sensors in CNC applications," *Sensors*, vol. 9, no. 5, pp. 3767–3789, 2009.

[18] Y. Sebsadji, S. Glaser, S. Mammar, and J. Dakhlallah, "Road slope and vehicle dynamics estimation," in *American Control Conference, 2008*, 2008, pp. 4603–4608.

[19] E. Todorov and M. I. Jordan, "A minimal intervention principle for coordinated movement," in *Proc. Adv. Neural Inf. Process. Syst.*, vol. 15, 2003, pp. 27–34.

[20] M. Yamakado and M. Abe, "An experimentally confirmed driver longitudinal acceleration control model combined with vehicle lateral motion," *Vehicle System Dynamics*, vol. 46, no. sup1, pp. 129–149, 2008.

[21] M. Yamakado and Y. Kadomukai, "A jerk sensor and its application to vehicle motion control systems," in *Proceedings of International Symposium of Automotive Technology & Automation*, vol. 27, 1994.

[22] M. Yamakado and M. Abe, "Examination of voluntary driving operational timing by using information obtained with the developed jerk sensor," in *FISITA 2006*, 2006.

[23] M. Yamakado, J. Takahashi, S. Saito, A. Yokoyama, and M. Abe, "Improvement in vehicle agility and stability by G-Vectoring control," *Vehicle System Dynamics*, vol. 48, no. sup1, pp. 231–254, 2010.